Desalination and Water Treatment
www.deswater.com
doi: 10.5004/dwt.2020.25529

جمعية علوم وتقنية المياه
Water Sciences and Technology Association

Synthesis and evaluation of nanocomposite forward osmosis membranes for Kuwait seawater desalination

Rajesha Kumar*, Mansour Ahmed, Garudachari, B., Jibu P. Thomas

Water Research Center, Kuwait Institute for Scientific Research, P.O. Box: 24885, 13109 Safat, Kuwait, Tel. +965 97920482; emails: ralambi@kisr.edu.kw (R. Kumar), mahmed@kisr.edu.kw (M. Ahmed), bgarudachari@kisr.edu.kw (B. Garudachari), jithomas@kisr.edu.kw (J. P. Thomas)

ABSTRACT

Multistage flash (MSF) and reverse osmosis (RO) are the two major desalination technologies currently serving the needs of freshwater in Kuwait. MSF is energy intensive and suffer from low water recovery, while RO desire energy to fulfil its pressure requirement for the process. Thus, globally the scientists are focusing on the innovative desalination technologies which could be operated at low cost and environmentally friendly. In this regard, forward osmosis (FO) is one such emerging technology which can be operated under "Non-Pressure" requirement conditions to reduce the energy/cost of the desalination process. The principle of FO involves flow of the pure water across the semipermeable membrane by maintaining an osmotic pressure gradient between the feed solution (low concentration solution) and draw solution (high concentration solution). Related to this concept, a project was conducted at Kuwait Institute for Scientific Research to fabricate potential and fouling control membranes for the FO desalination. The aim of this paper is to present the important outcomes of the project in fabricating different types of membranes and results related to the high-performance thin film nanocomposite (TFN) membranes obtained in the project compared with commercial FO membranes. The TFN membrane with 0.05 wt.% nanoparticle composition resulted in high flux of vs. the commercial CTA membrane. Therefore, this work concluded that a suitable selection of nanoparticles and their proper modification is essential to fabricate potential membranes for FO application. Further, a nano-based FO membrane showed a potential application in FO desalination compared with commercial FO membranes.

Keywords: Membrane fabrication; Flux; Reverse salt flux; Nanoparticles; Chemical modification

1. Introduction

At present world is facing the problem of water scarcity that is expected to grow worse soon. To meet this issue scientists are focusing on the innovative membrane technologies for the development of alternative water sources such as seawater desalination, and wastewater recovery (Shannon et al. 2008). Reverse osmosis (RO) desalination is the technical process designed to remove salts from the seawater to produce fresh water. The major factor influencing the selection of RO desalination technology is its high energy requirements. The total cost of desalination depends on energy (50%–70%), maintenance (20%–35%) and labor (10%–15%) costs. For Kuwait, a nonconventional water resource such as seawater is an absolute necessity to bridge the gap between supplies and demands. In Kuwait, the need of fresh water production by desalination is increased drastically. It means that the energy requirements for the process are also expected to increase by the same ratio. Forward osmosis is a novel, low-energy, and thus low-cost method for the desalination of seawater (Nicoll 2013). Unlike RO, it utilizes osmotic pressure gradient ($\Delta\pi$) as the driving force for the filtration of solute (salts) from the feed (seawater) (Fig. 1). Thus, no external pressure requirements made this process a less energy-consuming and low cost (Blandin et al. 2014). The fabrication of potential FO membranes is one of the major steps toward the optimization of FO desalination technology. Later, this technology itself can be integrated with RO or membrane distillation or nanofiltration to produce fresh water from seawater (Zaviska

* Corresponding author.

Presented at the 13th Gulf Water Conference – Water in the GCC: Challenges and Innovative Solutions. 12–14 March 2019, Kuwait

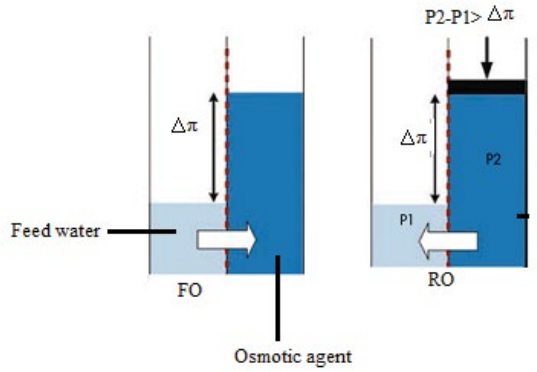

Fig. 1. Working principle of forward osmosis and reverse osmosis.

and Zou, 2014). The world's first FO desalination plant was developed by Modern Water technologies, in Oman during 2012. Currently, world-wide, the researchers are focusing on the mitigation of the major challenges in this field such as the development of low fouling and high flux membranes, and cost-effective draw solutions for the FO process.

Forward osmosis (FO) is one such emerging technology which gained more applications in water purification, seawater desalination, wastewater treatment, food processing, and pharmaceutical industry (Akther et al. 2015). It is an energy-efficient process that operates at low pressure or without additional pressure compared with RO. In FO, the water transport from dilute feed solution (FS) to the concentrated draw solution (DS) will take place through the semipermeable membrane (Huang et al. 2006). The driving force of FO comes from the osmotic pressure difference between the feed solution (FS) and draw solution (DS) separated by the membrane as presented in Fig. 1. The permeating water dilutes the DS, but only to a certain extent, that is, until an osmotic equilibrium is reached between the DS and the FS (Phuntsho et al. 2014). At the same time, there is a slow diffusion of solutes through the membrane from the DS to the FS due to the high concentration difference of ions between the two streams called as reverse solute flux (RSF). RSF not only reduces the effective osmotic driving force across the membrane but also increases the replenishment cost and scaling issue (Wang et al. 2015).

Advances in nanotechnology have led to the development of nano-structured materials, which may form the basis for novel FO membranes (Zaib and Fath 2013). From past one decade, the fabrication of different types of FO membranes especially in their thin film composite form was explored. Many studies have demonstrated that thin-film nanocomposite (TFN) membranes can be the solution to improve not only membrane water permeability but also antifouling resistance (Hamid et al. 2011). By incorporating a small quantity of hydrophilic nanomaterial into a polyamide (PA) layer is apparently able to improve characteristics of PA selective layer without compromising salt separation efficiency. Inorganic nano additives such as titanium dioxide (TiO_2), carbon nanotubes (CNTs), silica, silver, halloysites, and zeolite nanoparticles have contributed to improved flux and antifouling characteristics. A nano additive can improve PA film formation by offering the increased diffusion rate of monomers to the interface, increasing the hydrophilicity of the top PA surface and by reducing the roughness of the top PA surface formed (Ghosh et al. 2008). The entrapment of nanomaterial into the PA skin layer during interfacial polymerization is simpler and more effective when compared with the coating technique; since coating often results in pore plugging during fabrication process causing undesirable permeability characteristics.

Based on the above literature survey, this paper synthesizes nano-FO membranes and compares their performance with the commercial FO membranes. In the first stage, the fabrication of FO polymeric membranes by the chemical modification nanoparticles namely titanium dioxide (TiO_2), and halloysite nanotubes (HNT), was carried out while the carboxylic acid functionalized CNTs were directly purchased from Sigma-Aldrich Co. In the second stage, flat-sheet thin film nanocomposite FO membranes were fabricated, and their performance was evaluated in terms of flux. The study also includes the characterization of the membranes for surface hydrophilicity, morphology and roughness.

2. Experimental

2.1. Materials

The TiO_2 anatase powder, HNT and carboxylic acid functionalized CNT were procured from Sigma-Aldrich Co. The substrate polymer polysulfone (PSF) was procured from Sigma-Aldrich Co. All other solvents for the chemical modification and dope preparation were procured from Merck. For the membrane fabrication de-ionized water was used for phase inversion process.

2.2. Preparation of aminated titania nanotubes (ATNT) and dopamine modified HNT (PHNT)

The surface modification of TNTs was performed using silane coupling agent (3-aminopropyl) triethoxysilane (AAPTS) using literature reported procedure (Emadzadeh et al. 2015). Briefly, 2 g of TNTs was added to pure ethanol (25 mL) followed by 30 min sonication in bath. 0.5 g of APTES was added to the solution and stirred at 90°C for 4 h followed by filtration and subsequent washing using ethanol, ethanol/water (1:1 v/v), and water. The final products ATNTs were then dried at 100°C in a vacuum oven for 12 h. Fig. 14 presents the chemical structure of ATNTs.

The chemical modification of HNT was achieved using the procedure reported in the literature (Hebbar et al. 2016). HNT (10 mg/mL, 500 mL) was dispersed in DI water first by magnetic stirring for 15 min followed by ultra-sonication for 10 min. The base tris (hydroxymethyl) aminomethane was added to the HNT suspension until a pH of 8.8 was reached. Then, 0.2 mg/mL of dopamine powder was added to the HNT suspension and stirred at 30°C for 6 h. The product, polydopamine coated HNTs were collected by centrifugation and were washed with DI water for three more times (150 mL × 3). Finally, the brown coloured

DHNT was dried at 80°C for 10 h before using for characterization and membrane preparation.

2.3. General optimized procedure for the fabrication of thin film nanocomposite membranes

A thin film composite (TFC) membrane is composed of a thin selective layer of polyamide cast over the surface of substrate or support polymeric membrane layer. In the current work, the TFC membranes were fabricated via a two-step procedure.

2.4. General optimized procedure for the fabrication of substrate layer

Polymer (15.0 wt%) was taken in mixture of solvents DMF: NMP (62.25:20.75 wt%) at 26°C, and PEG (Mw = 600 Da, 2.0 wt%) was added at the same temperature. The mixture was stirred at 60°C for 4 h to obtain the homogeneous solution. The solution was degassed at 40°C for 2 h to remove the trapped air bubbles. The dope solution was poured onto a glass plate and casted by using a casting knife adjusted for the thickness of 150 μm. The glass plate was immediately immersed into a coagulation bath containing DI water at 25°C–26°C. After 20 min of coagulation process, the DI water was replaced with fresh water in the coagulation bath, and the membrane could stand for 24 h. Finally, the membrane was dried at 25°C–26°C.

2.5. General optimized procedure for the fabrication of polyamide layer by incorporating nanomaterial

The top active polyamide layer of TFN membrane was prepared by interfacial polymerization on the surface of a substrate layer. Nanomaterials in various concentrations (0.01, 0.05 and 0.1 w/v%, this concentration of nanomaterials was selected based on literature review) were dispersed in 2% (w/v) amine aqueous solution and sonicated for 2 h at 25°C–26°C followed by stirring for 30 min at the same temperature to avoid nanotubes agglomeration. The incorporation of nanomaterials into PA layer was carried out by taking the nanomaterials in aqueous amine solution due to their better dispersion. Amine aqueous solution was poured onto the top surface of the substrate, which was held horizontally for 2 min to ensure the penetration of amine solution into the pores of the substrate. The excess amine solution was then drained off from the substrate surface, and a rubber roller was employed to remove the residual droplets of amine solution. Now, 100 mL of 0.1% (w/v) acid solution in *n*-hexane was poured onto the substrate surface. The acid solution was drained off from the surface after 1 min contact time. After that, the TFN-FO membrane was cured at 80°C in an oven for 5 min. The unreacted amine and acid from the TFN membrane surface were removed by rinsing with pure *n*-hexane, and the membranes were dried at 25°C–26°C. All the prepared membranes were stored in a DI water container until they were tested.

2.6. Membrane characterization

The IR spectra of the modified nanoparticles were recorded using ATR-IR spectrometer from Bruker. The spectrum was recorded in the range of 600–4,000 cm^{-1} by directly placing the samples on the diamond prism followed by 32 scans. The TEM images of the modified TNTs were recorded using LVEM5 instrument (Delong America). The surface morphology of the membranes was recorded using Keysight 8500 field emission scanning electron microscope, and the imaging was conducted with back scattering electrons (BSE) mode to overcome charging effect. The surface contact angles of the membranes were recorded using optical contact angle and interface tension meter from USA KINO, model-SL200KB. The surface AFM images of the membranes were recorded using Concept Scientific Instrument (Nano-Observer), France, by scanning the membrane surface over 5 × 5 μm dimensions.

2.7. Determination of FO performance

FO experiments were conducted through a laboratory scale fabricated FO setup (Fig. 2). It consisted of PTFE cross-flow FO cell with outer dimensions of 12.7 × 10 × 8.3 cm (Sterlitech, USA), two pumps to maintain feed and DS flow (KNF, USA), and two flow meters (Blue-White Industries). The cross-flow velocity of both solutions was fixed at 8.0 cm/s, and the temperature was maintained at 25°C ± 0.5°C. The membrane coupons were inserted in the membrane cell in two different orientations: active layer facing the feed solution (AL-FS) mode and active layer facing the draw solution (AL-DS) mode. In this study, the aqueous solutions with concentrations of 2 M NaCl and 10 mM NaCl were used as draw and feed solutions, respectively. The high-performance membrane from each series was further subjected to flux and RSF study at two other concentrations of DS (0.5 M and 1.0 M). The FS concentration was maintained at same concentration of 10 mM NaCl to study the impact of DS concentrations on the flux as well as RSF values of the membranes. The water flux of the FO process, J (L/m^{2}h), was calculated from the volume changes of the draw solution and DI water using Eq. (1).

$$J = \frac{\Delta V}{A\Delta t} \tag{1}$$

where ΔV (L) is the volume change over a predetermined time Δt (h), and A is the effective membrane surface area (m^2).

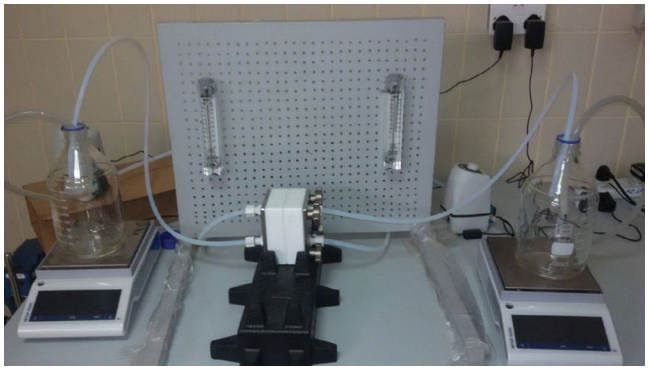

Fig. 2. Self-fabricated lab-scale FO performance test unit.

The RSF is a measure of the diffusion of draw solute to the feed solution during the FO process. To determine the RSF value, the concentration of back diffused DS was measured in terms of conductivity using a calibrated conductivity meter (ORION STAR A-221 model, Thermo Scientific). The RSF, J_s (gMH), was determined using Eq. (2).

$$J_s = \frac{\Delta C_t V_t}{A\Delta t} \quad (2)$$

where C_t (g/L) and V_t (L) are the reverse solute concentration and the volume of the feed solution, respectively, at an arbitrary time t.

3. Result and discussion

3.1. Characterization of ATNT and PHNT

3.1.1. FTIR analysis

For ATNT as shown in Fig. 3, a broad peak around 3,259 cm^{-1} is due to the $–NH_2$ of ATNT merged with the peak of partly unreacted –OH groups of TNT (Wang et al. 2013). The presence of two absorption peaks at 1,102 and 1,213 cm^{-1} correspond to stretching frequencies of Si–O and C–N, respectively. Meanwhile, the peak at 2,894 cm^{-1} is due to stretching vibration of Ti–O in modified TNTs (Niu and Cai, 2009).

Fig. 4 shows the ATR-IR spectra of the HNTs and PHNTs. The HNT spectrum showed absorption peaks at 3,694 and 3,625 cm^{-1} due to the stretching vibration of the –OH groups. The peak at 909 cm^{-1} attributed to the bending vibration of the Al–OH bonds and the spectral band at 1,020 cm^{-1} corresponds to the stretching vibration of Si–O bonds. Compared with HNT spectrum, the modified PHNT displayed additional bands at 1,496 and 1,615 cm^{-1} assigned to aromatic C-C stretching vibrations of symmetric and asymmetric modes, respectively (Gunasekaran et al. 2007). The PHNT spectrum displayed a broad peak in the range of 3,200–3,422 cm^{-1} corresponding to the –OH groups of the polydopamine. Also, additional peak appeared at 1,651 cm^{-1} corresponds to the carbonyl group of polydopamine confirmed the polydopamine surface modification of the HNTs.

The TEM images of the both ATNT and PHNTs are presented in Fig. 5. The image of ATNT and HNTs displayed

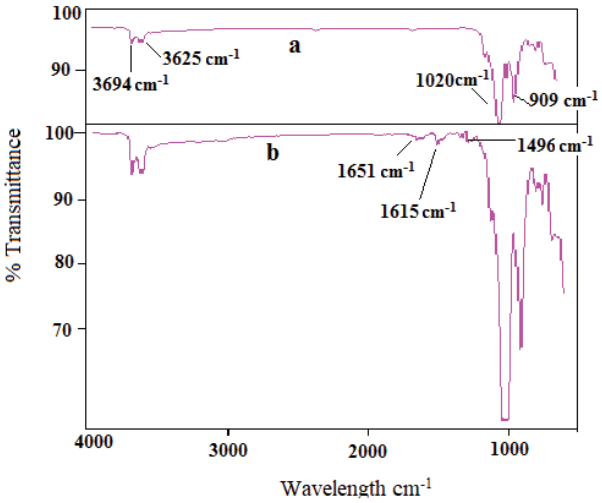

Fig. 4. FTIR spectra of HNT and PHNT.

tubular structures with varying length of 100 to 500 nm. The modification of HNTs resulted in thicker HNTs and increased the thickness of about 20–25 nm compared with neat HNTs. Overall, TEM results further supported the formation of polydopamine layer on the surface of the HNTs as observed by the previous researchers (Chao et al. 2013).

3.2. Characterization of membranes

3.2.1. Morphology of membranes

The surface images of TFN membranes clearly indicated the formation of porous ridge-valley structures by the loading of 0.05 wt% of CMWCNT, PHNT and ATNT into PA layers, respectively (Fig. 6). The chemical modification of nanoparticles enhanced the hydrophilicity of the nanoparticles which favoured the movement of nanoparticles to the surface of membranes during interfacial polymerization reaction to form polyamide layers. Hence, the loading of nanoparticles resulted in ridges and valley structures.

3.2.2. Roughness of the membranes

It is well known fact that the incorporation of nanoparticles into the PA layer will increase the surface roughness

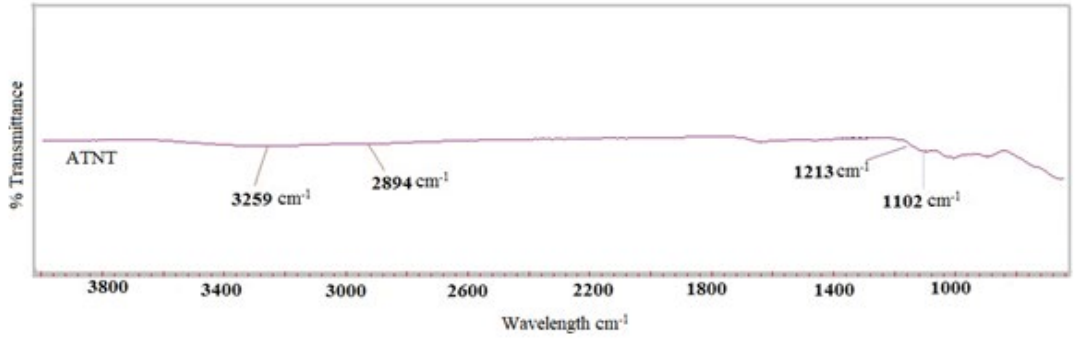

Fig. 3. FTIR spectra of ATNTs.

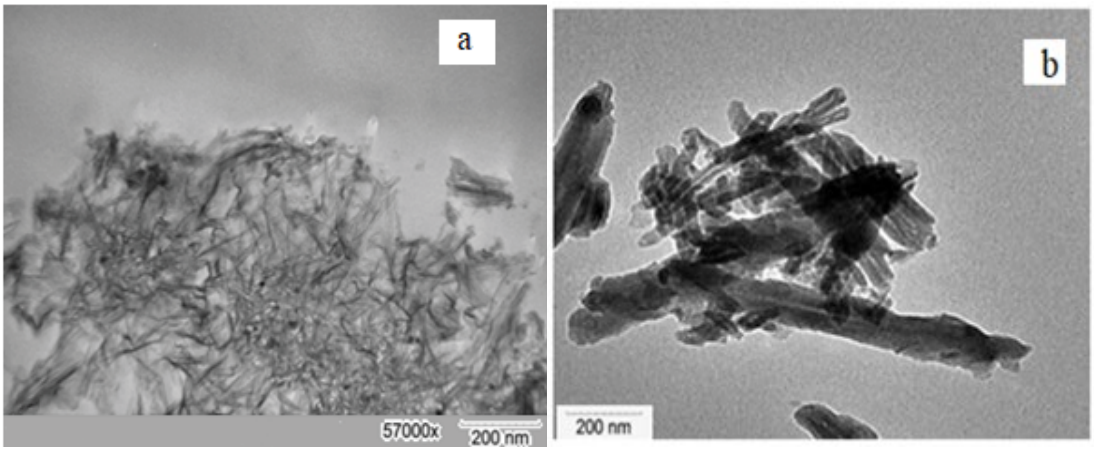

Fig. 5. TEM images of (a) ATNT and (b) PHNT.

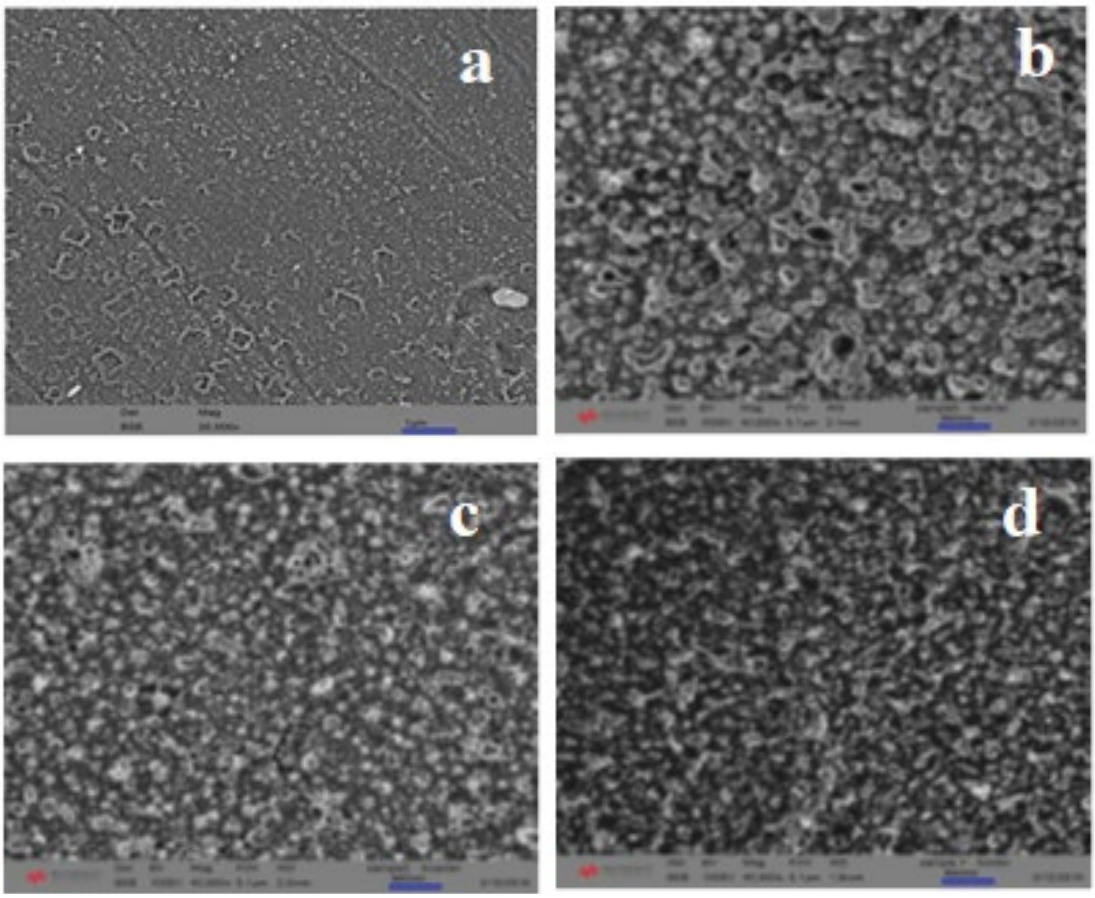

Fig. 6. Surface FESEM image of (a) control TFC membrane, (b) TFN-0.05 ATNT, (c) TFN-0.05 CCNT and (d) TFN-0.05 PHNT membranes.

values of the membranes. This could be explained by the fact that during the formation of PA layer via interfacial polymerization reaction the nanoparticles tend to partly agglomerate on the surfaces leading to more ridges and valleys as observed under SEM images. From Fig. 7, the increase in average roughness value is quite high for the loading of 0.05 wt% of CMWCNT might be due to quite higher hydrophobic characteristics of these nanoparticles compared with ATNT and PHNT.

3.2.3. *Hydrophilicity of membranes*

The lower value of contact angle signifies higher hydrophilicity of the membrane surface. The control TFC membrane

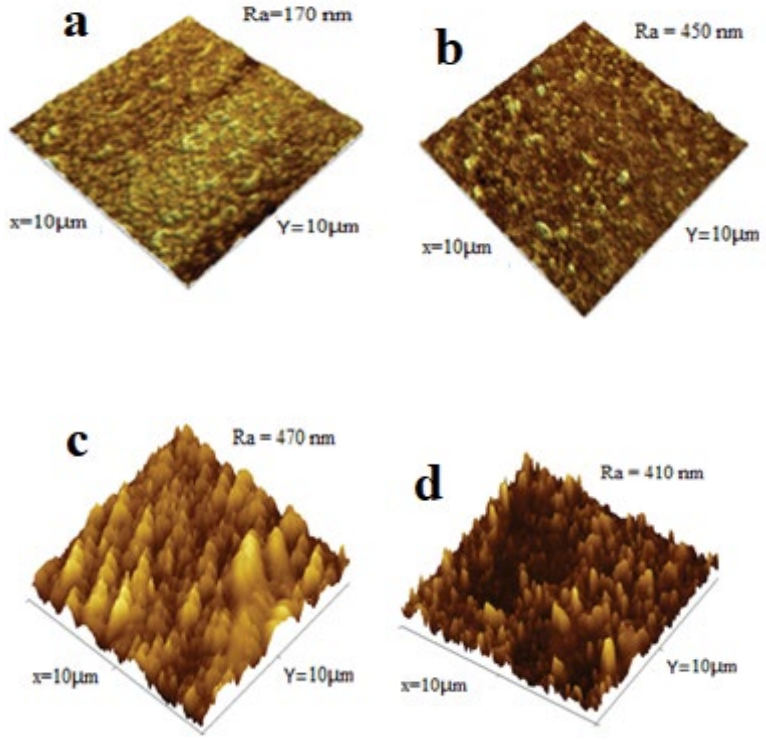

Fig. 7. Surface 3D AFM images of (a) control TFC membrane, (b) TFN-0.05 ATNT, (c) TFN-0.05 CMWCNT and (d) TFN-0.05 PHNT membranes.

Table 1
A detailed comparison of the FO performance between the different membranes prepared in this work and commercial FO membranes

Membrane	FO flux	PRO flux	RSF (g/m^2h)/FO	RSF (g/m^2h)/PRO	Remarks
HTI CTA flat sheet	13.5	25	5.0	10.4	Commercial cellulose acetate flat sheet FO membrane selected for comparative study
Sterlitech flat sheet	14	26.5	2	4.2	Commercial TFC FO membrane selected for comparative study
HTI TFC flat sheet	30	59	4	10	Commercial TFC FO membrane selected for comparative study
TFC control	12.2	20.4	2.8	4.3	Control TFC membrane
TFN-0.05ATNT	19.4	30.3	2.3	4.0	TFN membrane prepared by loading of 0.05 wt% ATNT into PA layer; produced high flux; relatively less RSF
TFN-0.05CMWCNT	18.2	28.6	2.8	3.7	TFN membrane prepared by the loading of 0.05 wt% CMWCNT into PA layer; produced high flux; relatively less RSF
TFN-0.05PHNT	17.6	28.4	3.2	4.8	TFN membrane prepared by the loading of 0.05wt% PHNT into PA layer; produced high flux; relatively less RSF

exhibited a contact angle of 59.02° and the loading of ATNT, PTNT and CMCNT has reduced the contact angle values to 53°, 52° and 56 °, respectively, representing least hydrophilicity of membrane with PHNT particles.

3.2.4. Membrane FO performance

The FO performance in terms of flux was improved by the loading of nanoparticles and 0.05 wt% loading was the optimized loading composition for any nanoparticles

selected in the study. The FO performance of the TFC control membrane and TFN membranes are presented in Table 1. Extra pores formed on the STNTs surfaces by sintering effect might create additional channels for the transport of water molecules. Also, the PHNTs possess tubular morphology and their incorporation into membrane matrix provided inner nano channels that improved the water flux (Hummer et al. 2001). This increased flux is due to the formation of new nano pathways created by nanotubes for the extra passage of water molecules (Emadzadeh et al. 2015). The presence of the water channel through the hollow nanotubes and the void between the nanotubes and polyamide matrix contributed to the improved flux of TFN membranes. The maximum flux was observed when active layer facing DS mode (PRO mode). This is due to the higher resistance offered by the top dense layer for the penetration of draw solute molecules in PRO mode (Amini et al., 2016). Though the RSF of the TFN membranes is higher than the TFC membrane, this increased RSF is much lower compared with drastic improvement in flux of the TFN membranes at both FO and PRO modes.

4. Conclusions

The nano-based FO membranes fabricated in this work demonstrated a better performance than commercial HTI CTA flat sheet and Sterlitech flat sheet membranes. The general optimized protocols were developed for the fabrication of different nano-based FO membranes. The characterization data provided the morphological, and chemical characteristics of the newly fabricated FO membranes in favour of FO desalination applications. The correlation study between membrane characterization and its performance result demonstrated the potentiality of the high-performance FO membrane towards their large-scale fabrication. The incorporation of modified ATNT, CMWCNT and PHNT with hydrophilic chemical functional groups into polyamide layer of TFN FO membranes improved the performed better than commercial FO membranes. However, most recently HTI, USA, was successful in commercializing cellulose triacetate based TFC membrane with a maximum FO flux 30 L/m^2 h and considered as the highest performer in FO desalination research. Hence, FO membrane fabrication work is not limited to the polymers selected in this project and a further research is recommended to identify the other polymers for potential FO membrane fabrication.

Acknowledgement

The authors are thankful to the Kuwait Institute for Scientific Research (KISR) for funding and supporting the implementation of this research work.

References

Akther, N., Sodiq, A., Giwa, A., Daer, S., Arafat, H. A., and Hasan, S. W., 2015, Recent advancements in forward osmosis desalination: A review". Chemical Engineering Journal, 281: 502–522.

Amini, M., Rahimpour, A., and Jahanshahi, M., 2016, "Forward osmosis application of modified TiO_2-polyamide thin film nanocomposite membranes". Desalination and Water Treatment. 57: 14013–14023.

Blandin, G., Verliefde, A. R. D., Tang, C. Y., and Le-Clecha, P. 2014. Opportunities to reach economic sustainability in forward osmosis–reverse osmosis hybrids for seawater desalination. Desalination, 363: 26–36.

Chao, C., Liu, J., Wang, J., Zhang, Y., Zhang, B., Zhang, Y., Xiang, X., and Chen, R., 2013, ACS Applied Material Interfaces. 5: 10559–10564.

Emadzadeh, D., Lau, W. J., Rahbari-Sisakht, M., Ilbeygi, H., Rana, D., Matsuura, T., and Ismail, A. F., 2015, "Synthesis, modification and optimization of titanate nanotubes polyamide thin film nanocomposite (TFN) membrane for forward osmosis (FO) application." Chemical Engineering Journal. 281: 243–251.

Emadzadeh, D., Lau, W. J., Rahbari-Sisakht, M., Ilbeygi, H., Rana, D., Matsuura, T., and Ismail, A. F., 2015, "Synthesis, modification and optimization of titanate nanotubespolyamide thin film nanocomposite (TFN) membrane for forward osmosis (FO) application." Chemical Engineering Journal. 281: 243–251.

Ghosh, A. K., Jeong, B.-H., Huang, X., and Hoek, E., 2008, "Impacts of reaction and curing conditions on polyamide composite reverse osmosis membrane properties." Journal of Membrane Science, 311(1): 34–45.

Gunasekaran, S., Kumar, R. T., and Ponnusamy, S., 2007, "Vibrational spectra and normal coordinate analysis of adrenaline and dopamine"., Indian Journal of Pure & Applied Physics. 45: 884–892.

Hamid, N., Ismail, A. F., Matsuura, T., Zularisam, A., Lau, W. J., Yuliwati, E., and Abdullah, M. S., 2011, "Morphological and separation performance study of polysulfone/titanium dioxide (PSF/TiO_2) ultrafiltration membranes for humic acid removal." Desalination, 273(1): 85–92.

Hebbar, R. S., Isloor, A. M., Anand, K., and Ismail, A. F., 2016, "Fabrication of polydopamine functionalized halloysite nanotube/polyetherimide membranes for heavy metal removal". Journal of Material Chemistry A. 4: 764–774.

Huang, X., Solasi, R., Zou, Y., Feshler, M., Reifsnider, K., Condit, D., Burlatsky, S., and Madden, T., 2006, "Mechanical endurance of polymer electrolyte membrane and PEM fuel cell durability." Journal of Polymer Science, Part B: Polymer Physics, 44: 2346–2357.

Hummer, G., Rasaiah, J. C., and Noworyta, J. P., 2001, "Water conduction through the hydrophobic channel of a carbon nanotube". Nature. 414: 188–190.

Nicoll, P., 2013, "Forward osmosis is not to be ignored" Desalination and Water Reuse (IDA), 22(4).

Niu, H., and Cai, Y., 2009, "Preparation of octadecyl and amino mixed group modified titanate nanotubes and its efficient adsorption to several ionic or ionizable organic analytes". Analytical Chemistry. 81: 9913–9920.

Phuntsho, S., Hong, S., Elimelech, M., and Shon, H. K., 2014, "Osmotic equilibrium in the forward osmosis process: Modelling, experiments and implications for process performance". Journal of Membrane Science, 453(1): 240–252.

Shannon, M. A., Bohn, P. W., Elimelech, M., Georgiadis, J. G., Marinas, B. J., and Mayes, A. M., 2008, "Science and technology for water purification in the coming decades". Nature, 452: 301–310.

Wang, L., Liu, W., Wang, T., and Ni, J., 2013, "Highly efficient adsorption of Cr(VI) from aqueous solutions by amino-functionalized titanate nanotubes". Chemical Engineering Journal. 225: 153–163.

Wang, P., Cui, Y., Ge, Q., Tew, T. F., and Chun, T. S., 2015, "Evaluation of hydroacid complex in the forward osmosis-membrane distillation (FO-MD) system for desalination". Journal of Membrane Science, 494(1): 1–7.

Zaib, Q., and Fath, H., 2013, "Application of carbon nano-materials in desalination processes". Desalination and Water Treatment, 51(1): 627–636.

Zaviska, F., and Zou, L., 2014, "Using modelling approach to validate a bench scale forward osmosis pre-treatment process for desalination". Desalination, 350: 1–13.